Materials Research Bulletin 46 (2011) 62–69

Contents lists available at ScienceDirect

Materials Research Bulletin

journal homepage: www.elsevier.com/locate/matresbu

Influence of the B-site ordering on the magnetic properties of the new $La_3Co_2MO_9$ double perovskites with M = Nb or Ta

V.C. Fuertes [a], M.C. Blanco [a], D.G. Franco [a], J.M. De Paoli [b], R.D. Sánchez [b,1], R.E. Carbonio [a,1,*]

[a] INFIQC (CONICET), Departamento de Fisicoquímica, Facultad de Ciencias Químicas, Universidad Nacional de Córdoba, Ciudad Universitaria, X5000HUA Córdoba, Argentina
[b] Centro Atómico Bariloche, CNEA and Instituto Balseiro, Universidad Nacional de Cuyo, Av. Bustillo 9500, 8400 Río Negro, Argentina

ARTICLE INFO

Article history:
Received 31 December 2009
Received in revised form 21 July 2010
Accepted 24 September 2010
Available online 2 November 2010

Keywords:
A. Ceramics
B. Chemical synthesis
C. X-ray diffraction
D. Crystal structure
D. Magnetic properties

ABSTRACT

Double perovskites $La_3Co_2NbO_9$ and $La_3Co_2TaO_9$ have been prepared by both solid state and sol–gel synthesis. The crystal structures have been studied from X-ray and neutron powder diffraction data. Rietveld refinements show that the crystal structure is monoclinic ($P2_1/n$), with different degrees of ordering of B′ and B″ cations, with octahedra tilted according to the Glazer notation $a^-b^-c^+$. Occupancy refinements show that the solid state materials are more B-site ordered than the sol–gel ones. Magnetization measurements show that these perovskites show two magnetic contributions, one with spontaneous magnetization and other with linear behaviour with the magnetic field associated to antiferromagnetic correlations. In the samples synthesized by solid state the spontaneous magnetization is more important than those synthesized by the sol–gel and present T_C of 62 K for Nb and 72 K for Ta. On the other hand, materials prepared by sol–gel have T_C 20 K for Nb and 40 K for Ta, respectively and major presence of the antiferromagnetic contribution. The competition between these magnetic behaviours is interpreted, by a microscopic point of view, as to be due to the different degrees of Co^{2+} ions disorder on the B site of the double perovskite structure. This disorder affects the ratio between the antiferromagnetic Co^{2+}–O–Co^{2+} and the ferromagnetic Co^{2+}–O–M^{5+}–O–Co^{2+} couplings proposed for the system.

1. Introduction

Perovskites have properties with very important technological applications like colossal magnetoresistance in $La_{1-x}Ca_xMnO_3$ [1], superconductivity in $BaBi_{1-x}Pb_xO_3$ [2], ferroelectricity in $BaTiO_3$ [3], piezoelectricity, magnetism, ion conductivity and many others. Because of these, perovskite compounds have shown to be one of the most highly versatile structures, principally because most of the elements of the periodic table can be accommodated in the A and/or B sites.

The unit cell in ABO_3 perovskite type materials can be seen like a three-dimensional corner-sharing network of BO_6 octahedra, with a large A cation occupying the 12 coordinate position between 8 BO_6 octahedra. If two atoms, B′ and B″, are placed on two crystallographic different B sites, a double perovskite is formed with the general formula $A_2B'B''O_6$ [4]. These B′ and B″ atoms can be ordered, or partially ordered. Ordering can be in a rock salt pattern, with different cations occupying alternating BO_6 octahedra or, rarely, it can form layers of alternating B cations. Ordering of the B cations occurs either when there is large size dissimilarity or when the charge difference is greater than 2 [4].

Both ABO_3 and $A_2B'B''O_6$ perovskites show several distortion mechanisms when the A-site cation is too small for the cuboctahedral cavity of the corner-sharing octahedral network [5]. Distortions arise from three mechanisms: cation displacements within the BO_6 octahedra and distortions and tiltings of these octahedra [6].

Besides the general formula $A_2B'B''O_6$, double perovskites can be written as $A_3B'_2B''O_9$ among many others. Usually, A is an alkali-earth ion, like Ca^{2+}, Sr^{2+}, Ba^{2+}. Materials in which alkali-earth cations A^{2+} had been partially replaced by Ln^{3+} lanthanide had been synthesized too. However, there are few reports of double perovskite materials in which the A site ion had been totally replaced by a small Ln^{3+} lanthanide [4,7–9].

Magnetic properties in double perovskites are strongly dependent on their B cations order–disorder relationship [10–13]. B-site ordered perovskites exhibit several different magnetic behaviours like ferromagnetism, ferrimagnetism, antiferromagnetism, magnetic frustration, spin glass, etc.

Magnetism in these compounds can be achieved when the B site is a transition metal cation with unmatched electrons. A really interesting ion is the d^7 Co^{2+} cation, which can make an important contribution to the magnetic moment. The lack of another

* Corresponding author. Tel.: +54 351 4334180; fax: +54 351 4334188.
E-mail address: carbonio@mail.fcq.unc.edu.ar (R.E. Carbonio).
[1] Members of the Research Career of CONICET.

0025-5408/$ – see front matter © 2010 Elsevier Ltd. All rights reserved.
doi:10.1016/j.materresbull.2010.09.033

paramagnetic ion inside a perovskite structure provides a clear sight for Co^{2+} magnetic interactions [6].

In a previous work we reported one member of this family: $La_3Co_2TaO_9$ prepared by solid state method [14]. In the present paper, we describe the synthesis, structural and magnetic characterization of the whole new double perovskites family: $La_3Co_2MO_9$ with M = Nb or Ta. The studied compounds have been synthesized by both traditional solid state and sol–gel methods. The second synthetic method allows us to obtain the same stoichiometric material at temperatures 400 °C below the synthesis temperature of the first one. Besides, we show the effect of the preparation method on the magnetic behaviour, which has not been extensively studied before for double perovskites.

2. Experimental

The $La_3Co_2MO_9$ phases (M = Nb or Ta) were synthesized as polycrystalline powders by both standard solid state and sol–gel method (tartrate-precursor decomposition). In the case of solid state method, stoichiometric amounts of La_2O_3, Co_3O_4 and M_2O_5 (M = Nb or Ta) in analytical grade were mixed, ground, placed in a platinum crucible and treated at 1400 °C in argon for 24 h with a 10% molar excess of Co, in order to compensate for Co volatilization. For the sol–gel method, M_2O_5 were previously dissolved by means of formation of a soluble complex of the corresponding metallic tartrates [15]. The starting materials M_2O_5 were dissolved in HF 48–51%P/V under a water bath with heating and agitation. When the complete dissolution of the oxide was reached, the heating was suspended and a solution of ammonium oxalate was added. The precipitation of a hydrated polynuclear oxide was produced by the drop of ammonia solution. The precipitate was filtered and washed with ammonia solution to ensure the complete elimination of fluorine. This obtained solid was fired at 1000 °C for 3 h, and weighted, to calculate the M_2O_5 concentration in the hydrous oxide ($M_2O_5 \cdot H_2O$) (M = niobium or tantalum). Finally, the required quantity of hydrous oxide was dissolved with tartaric acid and a small amount of hydrogen peroxide, under heating. A yellow solution in the case of niobium and a white one for tantalum were obtained. These solutions were mixed with $La(NO_3)_3 \cdot 6H_2O$ (Merck, 99% purity) and $Co(NO_3)_2 \cdot 6H_2O$ (Anedra, 98%) in stoichiometric amounts (except for the $Co(NO_3)_2 \cdot 6H_2O$ which was in a 10% mol excess to compensate for Co volatilization) and heated until the formation of a gel. The resulting pink precursor powders were dried for 24 h at 100 °C and subsequently heated 2 h at 300 °C and 10 h at 600 °C in air in order to eliminate organic compounds. Finally, the products were fired in a platinum crucible at 1000 °C during 24 h in an Ar inert atmosphere in order to stabilize the Co^{2+} cation.

The characterization by X-ray powder diffraction (XRPD) was performed using a Philips X'Pert Pro diffractometer (40 kV, 40 mA), in Bragg–Brentano reflection geometry with Cu Kα radiation (λ = 1.5418 Å). The data were obtained between 5° and 100° 2θ in steps of 0.02°. Neutron powder diffraction (NPD) patterns were collected at room temperature (RT) and 5 K in the D2B powder diffractometer at Institute Laüe-Langevin (ILL), Grenoble, France. The wavelength used was 1.5945 Å and the 2θ range was from 0.1° up to 159.9°, with increments of 0.05°.

The refinement of the crystal structure was performed by the Rietveld method [16] using the FULLPROF program [17]. A pseudo-Voigt shape function was always adequate to obtain good fits for experimental data.

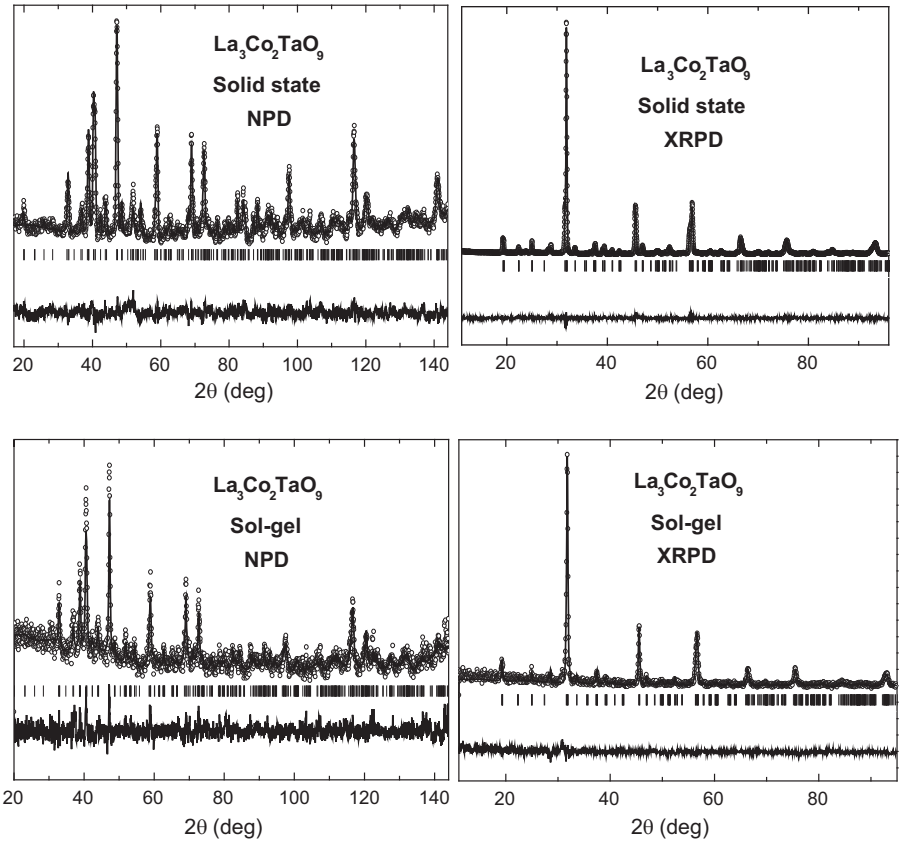

Fig. 1. Rietveld fits from neutron and X-ray powder diffraction patterns taken at room temperature for $La_3Co_2TaO_9$ compounds synthesized by solid state and sol–gel method, refined in the $P2_1/n$ space group. Experimental (circles), calculated (line) and difference (bottom solid line) profiles. Vertical bars represent positions of Bragg reflections for double perovskite.

The magnetic measurements were performed in a commercial superconducting quantum interference device magnetometer (SQUID) on powdered samples, in the 5–300 K temperature range and magnetic fields up to 5 T.

3. Results and discussion

3.1. Structural characterization

The neutron diffraction data were used in structural refinements for polycrystalline samples of both solid state and sol–gel synthesized $La_3Co_2MO_9$ compounds with M = Nb, Ta. Detected minor impurity phases, like $LaMO_4$ (M = Nb, Ta) and CoO are present in very low quantities (<2%). Rietveld refinements, Fig. 1, show that the structure of $La_3Co_2NbO_9$ and $La_3Co_2TaO_9$ can be well described with the monoclinic space group $P2_1/n$. The $LaMg_{2/3}Nb_{1/3}O_3$ crystal structure [18] was taken as the initial model for these compounds. Tables 1 and 2 summarized the refined structural data for the new perovskites at RT and at 5 K.

In this model, there are two crystallographic sites for B cations, 2d (1/2, 0, 0) and 2c (0, 1/2, 0), that allow an ordered arrangement for such ions. Only the solid state method $La_3Co_2TaO_9$ compound shows the most possible ordered arrangement for Co^{2+} and Ta^{5+} ions (the 2d site is fully occupied by Co), while the same compound prepared by sol–gel is much less ordered. In the case of $La_3Co_2NbO_9$ materials, Co^{2+} and Nb^{5+} ions are not in the most ordered possible arrangement but the solid state product is considerably more ordered than the sol–gel compound. This difference in the B-site order degree is then in consonance with the synthesis method used in these materials.

These perovskite compounds have a tolerance factor below one, 0.95 for both Nb and Ta cations because these ions have the same ionic radius. This factor is in agreement with the tilting of the $B'O_6$ and $B''O_6$ octahedra observed, since the ionic radius of La^{3+} is too small (Fig. 2). The tilt system for this space group is $a^-b^-c^+$. In the present work the octahedral tilts (δ) are calculated from B′–O–B″ bond angles (θ), as $(180-\theta)/2$ and are given in Tables 3 and 4. Transition metal–oxygen bond lengths for the four compounds are

Table 1
Lattice parameters, atomic positions, thermal factors and occupied fractions of $La_3Co_2NbO_9$ (synthesized by solid state and sol–gel method) at room temperature and 5 K as determined by neutron diffraction.

$La_3Co_2NbO_9$	Solid state		Sol–gel	
	RT[a]	5 K[b]	RT[c]	5 K[d]
Space group	$P2_1/n$	$P2_1/n$	$P2_1/n$	$P2_1/n$
a (Å)	5.5911(2)	5.5796(3)	5.5915(6)	5.5810(5)
b (Å)	5.6801(2)	5.6829(3)	5.6357(6)	5.6337(5)
c (Å)	7.9309(3)	7.9125(5)	7.9192(8)	7.9026(6)
β	89.982(1)	90.011(2)	90.027(5)	90.007(6)
A position (La^{3+})	4e	4e	4e	4e
x	0.4950(6)	0.4920(8)	0.4923(1)	0.4939(1)
y	0.5460(3)	0.5473(4)	0.5403(6)	0.5389(5)
z	0.2463(9)	0.2482(1)	0.2548(3)	0.2469(2)
B_{iso}	1.386(7)	1.519(1)	1.418(2)	1.872(1)
Frac. occ.	1.000(0)	1.000(0)	1.000(0)	1.000(0)
B′ position (Co^{2+}/Nb^{5+})	2d	2d	2d	2d
x	0.5000	0.5000	0.5000	0.5000
y	0.0000	0.0000	0.0000	0.0000
z	0.0000	0.0000	0.0000	0.0000
B_{iso}	0.58(1)	0.680(2)	0.418(2)	0.862(2)
Frac. occ.	0.457(2)/0.043(2)	0.457/0.043	0.416(4)/0.084(4)	0.416(4)/0.084(4)
B″ position (Co^{2+}/Nb^{5+})	2c	2c	2c	2c
x	0.0000	0.0000	0.0000	0.0000
y	0.5000	0.5000	0.5000	0.5000
z	0.0000	0.0000	0.0000	0.0000
B_{iso}	0.58(1)	0.680(2)	0.418(2)	0.862(2)
Frac. occ.	0.209(2)/0.291(2)	0.209/0.291	0.250(4)/0.250(4)	0.250(4)/0.250(4)
O(1) position	4e	4e	4e	4e
O(1) x	0.2985(6)	0.2935(1)	0.2853(9)	0.2840(9)
O(1) y	0.3037(4)	0.3083(6)	0.2921(9)	0.3064(7)
O(1) z	0.0370(4)	0.0347(5)	0.0339(9)	0.0341(4)
B_{iso}	0.56(3)	1.268(4)	2.302(6)	1.415(5)
Frac. occ.	1.000(0)	1.000(0)	1.000(0)	1.000(0)
O(2) position	4e	4e	4e	4e
O(2) x	0.2150(6)	0.2082(9)	0.2165(8)	0.2079(9)
O(2) y	0.7782(4)	0.7789(6)	0.7853(9)	0.7775(7)
O(2) z	0.0370(4)	0.0526(4)	0.0477(7)	0.0481(5)
B_{iso}	0.99(2)	1.020(3)	0.097(3)	0.148(3)
Frac. occ.	1.000(0)	1.000(0)	1.000(0)	1.000(0)
O(3) position	4e	4e	4e	4e
O(3) x	0.5797(3)	0.5826(4)	0.5751(7)	0.5763(6)
O(3) y	0.9837(3)	0.9821(4)	0.9883(5)	0.9870(4)
O(3) z	0.2493(7)	0.2450(8)	0.2597(9)	0.2591(9)
B_{iso}	0.86(2)	1.192(2)	0.925(3)	1.223(2)
Frac. occ.	1.000(0)	1.000(0)	1.000(0)	1.000(0)

[a] $\chi^2 = 0.599$; for $\lambda = 1.594$ Å, $wRp = 13.6$, $Rp = 14.1$; Bragg R-factor = 6.87.
[b] $\chi^2 = 0.726$; for $\lambda = 1.594$ Å, $wRp = 19.0$, $Rp = 19.9$; Bragg R-factor = 11.4.
[c] $\chi^2 = 0.403$; for $\lambda = 1.594$ Å, $wRp = 20.3$, $Rp = 22.9$; Bragg R-factor = 9.16.
[d] $\chi^2 = 0.708$; for $\lambda = 1.594$ Å, $wRp = 14.8$, $Rp = 15.7$; Bragg R-factor = 9.69.

Table 2
Lattice parameters, atomic positions, thermal factors and occupied fractions of $La_3Co_2TaO_9$ (synthesized by solid state and sol–gel method) at room temperature and 5 K as determined by neutron diffraction.

$La_3Co_2TaO_9$	Solid state		Sol–gel	
	RT[a]	5 K[b]	RT[c]	5 K[d]
Space group	$P2_1/n$	$P2_1/n$	$P2_1/n$	$P2_1/n$
a (Å)	5.6002(5)	5.5873(5)	5.6061(9)	5.5953(9)
b (Å)	5.6919(5)	5.6920(5)	5.6587(9)	5.654(1)
c (Å)	7.9426(6)	7.9239(7)	7.9447(9)	7.928(1)
β	89.970(5)	90.003(7)	89.977(6)	89.944(6)
A position (La^{3+})	4e	4e	4e	4e
x	0.4956(7)	0.4908(6)	0.5131(6)	0.4969(7)
y	0.5454(3)	0.5454(3)	0.5380(3)	0.5409(3)
z	0.2463(8)	0.2527(9)	0.2598(7)	0.2343(5)
B_{iso}	1.935(4)	1.300(4)	2.157(5)	2.06(5)
Frac. occ.	1.000(0)	1.000(0)	1.000(0)	1.000(0)
B′ position (Co^{2+}/Ta^{5+})	2d	2d	2d	2d
x	0.5000	0.5000	0.5000	0.5000
y	0.0000	0.0000	0.0000	0.0000
z	0.0000	0.0000	0.0000	0.0000
B_{iso}	0.702(9)	0.342(8)	1.000(5)	0.13
Frac. occ.	0.500(0)	0.500(0)	0.262(4)/0.238(4)	0.262/0.238
B″ position (Co^{2+}/Ta^{5+})	2c	2c	2c	2c
x	0.0000	0.0000	0.0000	0.0000
y	0.5000	0.5000	0.5000	0.5000
z	0.0000	0.0000	0.0000	0.0000
B_{iso}	0.702(9)	0.342(8)	1.000(5)	0.13
Frac. occ.	0.167/0.333	0.167/0.333	0.405(4)/0.095(4)	0.405/0.095
O(1) position	4e	4e	4e	4e
O(1) x	0.2933(9)	0.2846(9)	0.3026(9)	0.3071(9)
O(1) y	0.3058(8)	0.3062(9)	0.3099(9)	0.3085(9)
O(1) z	0.0366(7)	0.0421(9)	0.0454(9)	0.046(1)
B_{iso}	1.397(5)	1.451(6)	0.13(8)	0.29
Frac. occ.	1.000(0)	1.000(0)	1.000(0)	1.000(0)
O(2) position	4e	4e	4e	4e
O(2) x	0.2117(9)	0.2054(9)	0.225(1)	0.2199(9)
O(2) y	0.7751(8)	0.7873(8)	0.782(1)	0.778(1)
O(2) z	0.0519(6)	0.0413(9)	0.024(1)	0.032(1)
B_{iso}	1.132(4)	0.034(0)	2.3(1)	2.1(2)
Frac. occ.	1.000(0)	1.000(0)	1.000(0)	1.000(0)
O(3) position	4e	4e	4e	4e
O(3) x	0.5825(5)	0.5844(6)	0.5887(9)	0.5724(9)
O(3) y	0.9866(5)	0.9856(5)	0.9801(9)	0.9761(9)
O(3) z	0.2468(9)	0.2614(9)	0.2479(9)	0.253(2)
B_{iso}	1.043(2)	0.779(2)	0.07(8)	1.0(1)
Frac. occ.	1.000(0)	1.000(0)	1.000(0)	1.000(0)

[a] $\chi^2 = 0.462$; for $\lambda = 1.594$ Å, $wRp = 21.9$, $Rp = 24.5$; Bragg R-factor = 9.28.
[b] $\chi^2 = 0.739$; for $\lambda = 1.594$ Å, $wRp = 23.0$, $Rp = 23.7$; Bragg R-factor = 13.5.
[c] $\chi^2 = 0.437$; for $\lambda = 1.594$ Å, $wRp = 36.0$, $Rp = 42.0$; Bragg R-factor = 11.3.
[d] $\chi^2 = 0.476$; for $\lambda = 1.594$ Å, $wRp = 35.3$, $Rp = 38.8$; Bragg R-factor = 16.0.

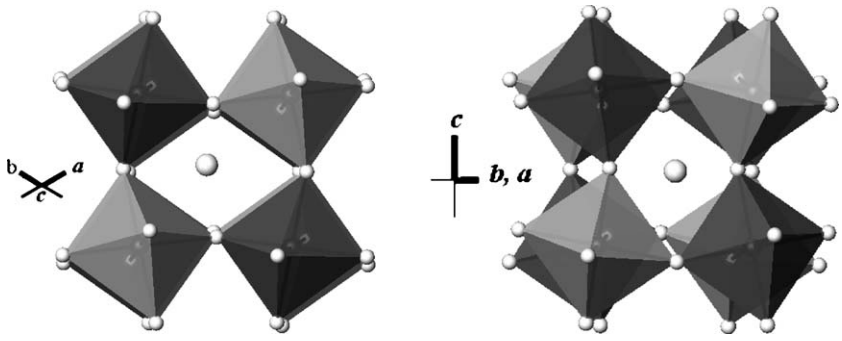

Fig. 2. Projections along the primitive axes of the crystal structure of $La_3Co_2MO_9$ (M = Nb or Ta) showing in phase (a) and out-of-phase (b) rotations of the BO_6 octahedra. Octahedra with small spheres in the corners represent CoO_6 (dark grey) and MO_6 (light grey), where M = Nb^{5+} or Ta^{5+}. Isolated spheres are La^{3+} ions.

Table 3
Selected distances and angles of $La_3Co_2NbO_9$ (synthesized by solid state and sol–gel method) at room temperature and 5 K as determined by neutron diffraction. Tilt angles have been calculated as: $\delta = (180 - \theta)/2$.

$La_3Co_2NbO_9$	Temperature	Distances (Å)		Angles (°)	Tilt angles (°) (δ)
		(Co1/Nb1)–O1	(Co2/Nb2)–O1	(Co1/Nb1)–O1–(Co2/Nb2)	
		(Co1/Nb1)–O2	(Co2/Nb2)–O2	(Co1/Nb1)–O2–(Co2/Nb2)	
		(Co1/Nb1)–O3	(Co2/Nb2)–O3	(Co1/Nb1)–O3–(Co2/Nb2)	
Solid state	300 K	2 × 2.029(3)	2 × 2.081(3)	151.7(1)	14.2
		2 × 2.025(3)	2 × 2.069(3)	153.5(1)	13.3
		2 × 2.039(5)	2 × 2.029(7)	154.2(2)	12.9
	5 K	2 × 2.115(4)	2 × 1.986(4)	152.4(2)	13.8
		2 × 2.098(4)	2 × 2.009(4)	151.7(2)	14.2
		2 × 1.995(6)	2 × 2.072(6)	153.2(2)	13.4
Sol–gel	300 K	2 × 2.055(8)	2 × 1.997(9)	156.8(4)	11.6
		2 × 2.030(7)	2 × 2.047(7)	153.6(3)	13.2
		2 × 2.100(8)	2 × 1.950(8)	155.7(3)	12.2
	5 K	2 × 1.993(6)	2 × 2.123(5)	154.5(2)	12.8
		2 × 1.984(5)	2 × 2.091(5)	153.3(2)	13.4
		2 × 1.952(7)	2 × 2.092(7)	155.3(2)	12.4

also displayed. We attempted to refine site-occupancy parameters for oxygen atoms and cations but they did not significantly vary, then, such parameters were fixed to unity.

3.2. Magnetic characterization

The $La_3Co_2MO_9$ compounds, which have been synthesized by solid state method, display spontaneous magnetization at low temperature, Fig. 3, top left side. Below, the inverse of the magnetic susceptibility calculated by mol of Co^{2+} ions is also plotted. The paramagnetic region is not completely linear (as it is observed in some ferrimagnetic materials). We fit with a Curie–Weiss law (in the 200–300 K interval) and the obtained θ values are 41.7(2) K for Ta^{5+} compound and 36.2(5) K for Nb^{5+} sample. Note that we obtained positive θ values, which have been observed previously for other ferrimagnetic double perovskites, like Sr_2FeMoO_6. As an example of this, Tovar et al. [19], have obtained $\theta = 446$ K for Sr_2FeMoO_6. Consequently, our positive θ values show that ferromagnetic interactions can be predominant in this system. Taking the derivative of M vs T data it is possible to define a minimum which is associated with the ordering temperature T_C (inset of the upper left figure), 72(2) K for Ta sample and 62(2) K for Nb case. From the slope of the Curie–Weiss fit, the μ_{eff} values are 3.82(5) and 3.79(5)μ_B for Ta^{5+} and Nb^{5+} compounds, respectively per Co^{2+} mol. Both are in good agreement with the 3.87μ_B expected for Co^{2+} (HS, $S = 3/2$) with spin-only contribution to the magnetic moment.

The M vs H curves (Fig. 3 left side bottom) show a marked hysteresis in the whole range of magnetic fields. In both samples, linear M vs H dependence is observable at low and high magnetic fields, where a complete saturation expected for the Co^{2+}(HS) ions (3μ_B) is not reached. This behaviour suggests at least that two different magnetic interactions may be coexisting in the samples.

On the other hand the $La_3Co_2MO_9$ compounds synthesized by sol–gel methods (Fig. 3 right side) present differences with respect to the solid state compounds previously described. The sol–gel samples also display spontaneous magnetization, below 40 K when M = Ta, and below 20 K when M = Nb, but in this case the corresponding obtained θ values are negative, −90(2) K for Ta^{5+} compound and −28(2) K for Nb^{5+} sample, which indicates that antiferromagnetic interactions play a predominant role. M vs H hemicycles for sol–gel series are shown in Fig. 3, bottom right side. Here, in the magnetic ordered region at low temperatures the spontaneous contribution is significantly weaker than that for the solid state case. In fact, the saturation magnetization is not even reached at 5 K and 5 T and these curves are more linear that those for the samples prepared at more high temperatures by the solid state method. Moreover, the μ_{eff} values are 5.37(5) and 4.27(5)μ_B per Co^{2+} mol for Ta^{5+} and Nb^{5+} compounds, respectively, indicating the presence of unquenched orbital moment contribution for Co^{2+} (HS). The corresponding theoretical value is 6.63μ_B for spin–orbit contribution to magnetic moment. Such unquenched Co^{2+} (HS) is consistent with other Co containing ordered antiferromagnetic double perovskites [20–24].

It is interesting to note that solid state samples show spin only contribution to the magnetic moment while sol–gel compounds possess unquenched orbital contribution. It has been stated that

Table 4
Selected distances and angles of $La_3Co_2TaO_9$ (synthesized by solid state and sol–gel method) at room temperature and 5 K as determined by neutron diffraction. Tilt angles have been calculated as: $\delta = (180 - \theta)/2$.

$La_3Co_2TaO_9$	Temperature	Distances (Å)		Angles (°)	Tilt angles (°) (δ)
		(Co1/Ta1)–O1	(Co2/Ta2)–O1	(Co1/Ta1)–O1–(Co2/Ta2)	
		(Co1/Ta1)–O2	(Co2/Ta2)–O2	(Co1/Ta1)–O2–(Co2/Ta2)	
		(Co1/Ta1)–O3	(Co2/Ta2)–O3	(Co1/Ta1)–O3–(Co2/Ta2)	
Solid state	300 K	2 × 2.110(5)	2 × 2.001(6)	152.3(2)	13.9
		2 × 2.101(6)	2 × 2.007(5)	152.7(2)	13.7
		2 × 2.016(8)	2 × 2.065(8)	153.5(3)	13.3
	5 K	2 × 1.964(7)	2 × 2.144(7)	152.2(3)	13.9
		2 × 2.024(5)	2 × 2.069(6)	153.9(2)	13.1
		2 × 1.950(7)	2 × 2.126(7)	152.8(3)	13.6
Sol–gel	300 K	2 × 2.11(1)	2 × 2.04(1)	147.8(4)	16.1
		2 × 1.98(1)	2 × 2.04(2)	163.1(5)	8.5
		2 × 2.11(2)	2 × 1.99(2)	151.2(6)	14.4
	5 K	2 × 2.083(8)	2 × 2.063(9)	147.2(3)	16.4
		2 × 2.03(1)	2 × 2.01(1)	160.5(5)	9.8
		2 × 2.06(1)	2 × 2.02(2)	152.7(6)	13.7

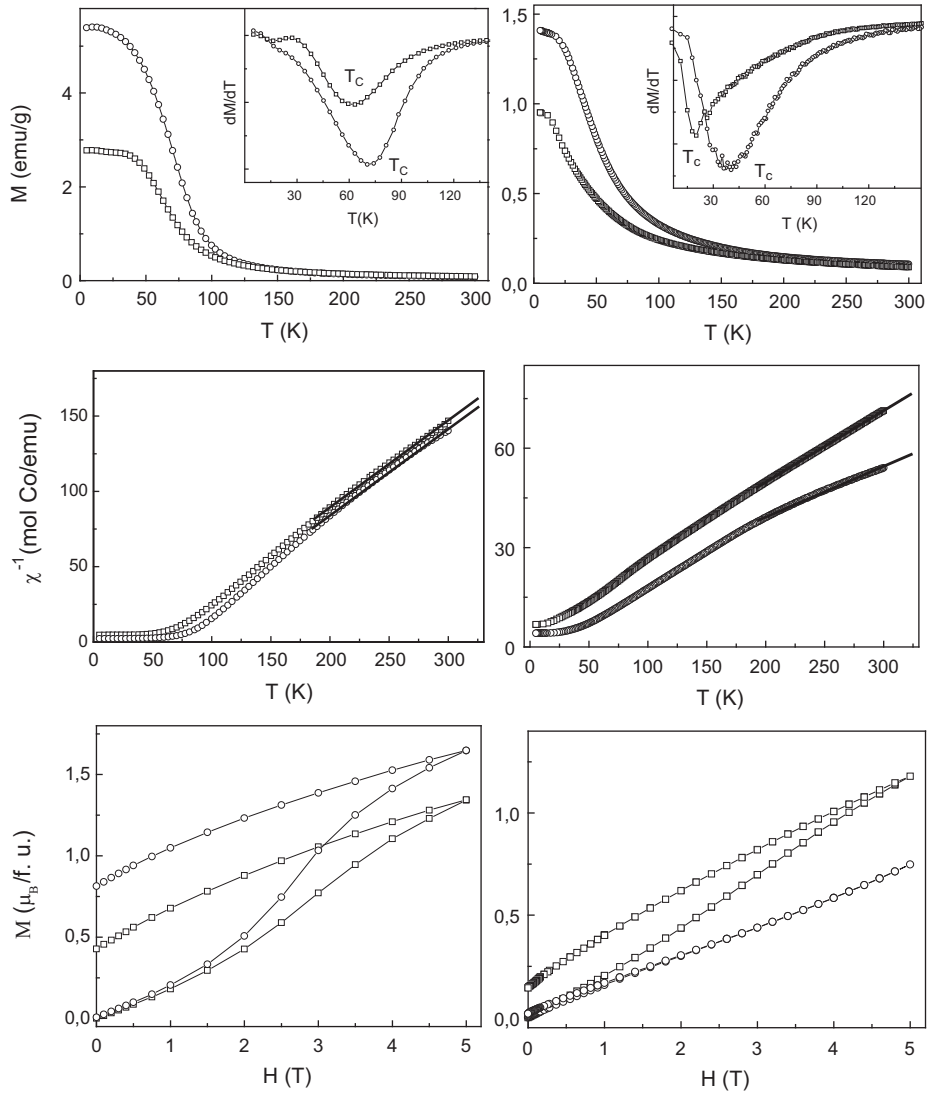

Fig. 3. Magnetization (M) vs T; reciprocal susceptibility (χ^{-1}) vs T both in the 5–300 K interval at H = 5 kOe; and M vs applied magnetic field (H) in the 0–5 T range at 5 K for $La_3Co_2MO_9$ (M = Nb and Ta) samples synthesized by solid state method (left side) and sol–gel method (right side). Experimental data: Ta compounds (circles) and Nb compounds (squares). Full lines represent fit to Curie–Weiss law. Inset: dM/dT vs T shows the transition temperature.

Co^{2+} is expected to have sizable orbital contribution to the magnetic moment [25]. In fact, it has been observed by some of the authors of the present paper for several Co containing double perovskites [20,22,23] that Co^{2+} has a large unquenched orbital contribution to the magnetic moment. However, it is not completely clear in the literature why some Co^{2+} compounds have very large orbital contribution and other have less or none. Some authors correlate unquenched orbital contribution with polyhedra not strongly distorted [21], however in our case there are not important differences between the octahedra of the different samples (see Tables 3 and 4). We must however take into consideration, that in all the published cases of orbital contribution in Co containing double perovskites [20–24], the samples are highly B-site ordered antiferromagnetic double perovskites. In our case, the antiferromagnetic double perovskites (the sol–gel ones) have magnetic orbital contribution, on the other hand, the "ferrimagnetic" ones (those prepared by solid state) show no orbital contribution. Even if this is not a "fundamental" explanation, is the only "empirical" correlation we could find.

The M vs H curves and the obtained θ values (positive and negative) evidence, for both $La_3Co_2MO_9$ synthesized compounds, solid state and sol–gel, that two magnetic contributions are present in the system with different degrees of the same effect. The non linear paramagnetic χ^{-1} vs T curves, and also the resultant spontaneous contributions in the M vs H curves indicate ferrimagnetic behaviour, on the other hand, the linear contribution observed in the M vs H curves can be associated to antiferromagnetic contribution which is more predominant in the sol–gel samples than in the solid state compounds. This dissimilar behaviour depending on the preparation method (which governs the order–disorder of the B sites) would indicate a competition between both types of magnetic interactions, which will prevail depending on the B-site ordering.

According to this correlation of the predominant magnetic interactions with the order–disorder of the B sites, we try to find a simple model to explain these results. Fig. 4 shows the two possible extreme situations originated from a crude two-dimensional statistical study. The first possibility (Fig. 4a) is the completely disordered material which does not show any difference between two crystallographic B sites and which can be written as $La(Co_{2/3}M_{1/3})_{2c}(Co_{2/3}M_{1/3})_{2d}O_3$. The other option is the most ordered possible structure (Fig. 4b) and this is specifically the case for $La_3Co_2TaO_9$ solid state method synthesized compound, which can be written as $La(Co_{1/3}Ta_{2/3})_{2c}(Co)_{2d}O_3$

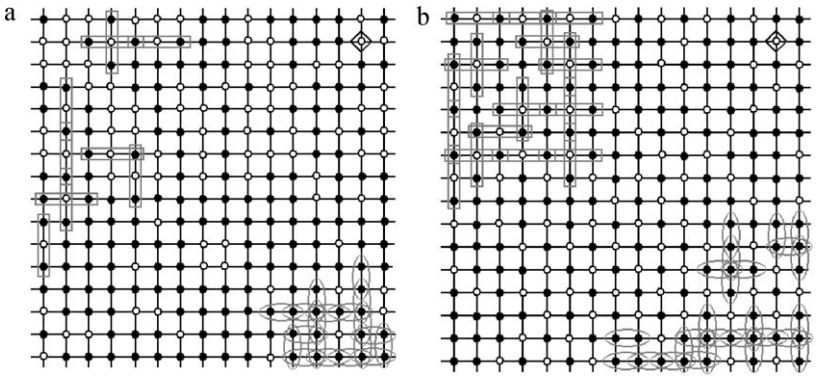

Fig. 4. Schematic representation of 2D-random arrangement of Co^{2+} and M^{5+} ions for the crystal structure of $La_3Co_2MO_9$ with: (a) complete antisite disorder of B type cations, (b) the most ordered arrangement of B type cations. Co^{2+} (full circles), M^{5+} (empty circles), BO_6 octahedra (black rhombus), La^{3+} and O^{2-} ions are omitted for simplicity. Some of the Co–O–Co antiferromagnetic couplings are indicated with grey ovals and the Co–O–M–O–Co ferromagnetic ones with grey rectangles.

[14]. Note that these two-dimensional analyses do not take into account octahedral distortion or tilting. In Fig. 4, some Co^{2+}–O–Co^{2+} superexchange couplings are pointed through grey ovals while some long range couplings (Co^{2+}–O–M^{5+}–O–Co^{2+}) are shown through grey rectangles. All these interactions were counted and the ratio Co^{2+}–O–M^{5+}–O–Co^{2+}/Co^{2+}–O–Co^{2+} was calculated for both cases. In the case of the completely disordered arrangement the ratio was approximately 0.25, while in the most possible ordered arrangement the ratio was approximately one. Thus, in most ordered solid state compounds the Co^{2+}–O–M^{5+}–O–Co^{2+} long range interactions are predominant and the behaviour is ferromagnetic, while in sol–gel compounds Co^{2+}–O–Co^{2+} antiferromagnetic superexchange couplings govern the magnetic interactions. The Co^{2+}–O–M^{5+}–O–Co^{2+} couplings could be ferromagnetic due to partial electronic density transference from Co^{2+} ions to empty d orbitals of d^0 M^{5+} cation, with parallel spins, according to highest multiplicity Hund's rule. Nb^{5+} and Ta^{5+} belong to the class of highly charged d^0 cations where the separation between the HOMO (Highest Occupied Molecular Orbitals) and LUMO (Lowest Unoccupied Molecular Orbitals) states is sufficiently small so as to permit a mixing between them [26]. Since HOMO are mainly anionic (oxygen 2s and 2p) and LUMO mainly cationic, arising from empty d states, this mixing between HOMO and LUMO in turn means that some partial charge transfer from s–p oxygen orbitals to d orbitals of the transition metals is occurring, allowing thus the ferromagnetic couplings between Co^{2+} mediated by M^{5+}. The Goodenough–Kanamori rules [27] state that superexchange interactions are antiferromagnetic when the electron transfer is between overlapping orbitals that are both half-filled, but they are ferromagnetic when the electron transfer is from a half-filled to an empty orbital like is this case.

4. Conclusions

New materials from the double perovskite family whose stoichiometric compositions are $La_3Co_2MO_9$ with M = Nb and Ta, have been successfully synthesized by both solid state and sol–gel methods. These compounds could be refined in $P2_1/n$ space group. Their tilting system is $a^-b^-c^+$. The solid state method synthesized compounds have shown to be more B-site ordered than sol–gel synthesized compounds and this is the cause for the quite different magnetic behaviours. From the magnetic measurements at high temperatures the calculated Co^{2+} effective magnetic moments are 3.82(5) and 3.79(5)μ_B for Ta^{5+} and Nb^{5+} compounds, respectively in solid state samples and 5.37(5) and 4.27(5)μ_B for Ta^{5+} and Nb^{5+} compounds, respectively, for sol–gel samples. At low temperatures, solid state materials show spontaneous magnetization below T_C = 72 K for Ta^{5+} and 62 K for Nb^{5+} compounds and positive θ values. While the sol–gel materials with T_C = 40 K and 20 K, for Ta^{5+} and Nb^{5+} compounds, respectively, present low spontaneous magnetization values and negative θ values. This behaviour can be understood in the frame of ferrimagnetic materials with a background of Co^{2+}–O–Co^{2+} antiferromagnetic superexchange couplings that competes with ferromagnetic Co^{2+}–O–M^{5+}–O–Co^{2+} arrangements. The solid state compounds show a "more" ferromagnetic behaviour than the sol–gel ones, which are "more" antiferromagnetic. This difference in magnetic behaviour, also shown in the *M* vs *H* experiments, can be explained by a simple model which shows that the most B-site ordered solid state compounds favors the ferromagnetic Co^{2+}–O–M^{5+}–O–Co^{2+} arrangements more than in the sol–gel case, where the antiferromagnetic superexchange couplings Co^{2+}–O–Co^{2+} are predominant.

Acknowledgements

V.C.F. thanks Ana Gabriela Leyva for the useful observations and contributions.

R.E.C. thanks ANPCYT (PICT2007 00303), CONICET and SECYT-UNC for financial support. D.G.F. and J.M.D.P. thank CONICET for fellowships. R.D.S. thanks ANPCyT (PICT 2004-21372) and Sectyp-UNCu (06/C324). We gratefully acknowledge Institut Laüe Langevin (ILL) (Grenoble, France) for access to D2B line.

References

[1] B.T. Cong, P.N.A. Huy, N.H. Long, J. Magn. Mater. 262 (2003) 437.
[2] D.T. Marx, P.G. Radaelli, J.D. Jorgensen, R.L. Hitterman, D.G. Hinks, S. Pei, B. Dabrowski, Phys. Rev. B 46 (1992) 1144–1156.
[3] B.D. Stojanovic, C. Javalekic, V. Vukotic, A.Z. Simoes, J.A. Varela, Ferroelectrics 319 (2005) 291.
[4] K.L. Holman, Q. Huang, T. Klimczuk, K. Trzebiatowski, J.W.G. Bos, E. Morosan, J.W. Lynn, R.J. Cava, J. Solid State Chem. 180 (2007) 75.
[5] M.W. Lufaso, P.W. Barnes, P.M. Woodward, Acta Crystallogr. B 62 (2006) 397.
[6] L. Ortega San Martín, J.P. Chapman, L. Lezama, J. Sánchez-Marcos, J. Rodríguez-Fernández, M.I. Arriortua, T. Rojo, J. Mater. Chem. 15 (2005) 183.
[7] G. Blasse, J. Inorg. Nucl. Chem. 27 (1965) 993.
[8] Q. Lin, M. Greenblatt, M. Croft, J. Solid State Chem. 179 (2006) 2086–2092.
[9] S.A. Ivanov, N.W. Thomas, S. Ananta, R. Tellgren, H. Rundlof, J. Eur. Ceram. Soc. 20 (2000) 2325–2329.
[10] L. Bufaiçal, L. Mendonça Ferreira, R. Lora-Serrano, P.G. Pagliuso, A. Caytuero, E. Baggio-Saitovich, Physica B 404 (2009) 3285–3288.
[11] A.S. Ogale, S.B. Ogale, R. Ramesh, T. Venkatesan, Appl. Phys. Lett. 75 (1999) 537–539.
[12] Ll. Balcells, J. Navarro, M. Bibes, A. Roig, B. Martínez, J. Fontcuberta, Appl. Phys. Lett. 78 (2001) 781–783.
[13] M.C. Viola, M.S. Augsburger, R.M. Pinacca, J.C. Pedregosa, R.E. Carbonio, R.C. Mercader, J. Solid State Chem. 175 (2003) 252–257.
[14] V.C. Fuertes, M.C. Blanco, D.G. Franco, J.M. De Paoli, E.V. Pannunzio-Miner, R.D. Sánchez, M.T. Fernández-Díaz, R.E. Carbonio, Physica B 404 (2009) 2717–2719.
[15] R.N. Das, P. Pramanik, Mater. Lett. 46 (2000) 7–14.
[16] H.M. Rietveld, J. Appl. Crystallogr. 2 (1969) 65.

[17] J. Rodríguez-Carvajal, Physica B 192 (1993) 55.
[18] I.K. Choi, B.J. Cho, J.H. Paik, S. Nahm, J.S. Kim, H.-J. Lee, H.-M. Parck, J.D. Byun, B.-G. Ahn, Mater. Res. Bull. 35 (2000) 921–928.
[19] M. Tovar, M.T. Causa, A. Butera, J. Navarro, B. Martínez, J. Fontcuberta, M.C.G. Passeggi, Phys. Rev. B 66 (2002) 024409.
[20] M.C. Viola, M.J. Martínez-Lope, J.A. Alonso, J.L. Martínez, J.M. De Paoli, S. Pagola, J.C. Pedregosa, M.T. Fernández-Díaz, R.E. Carbonio, Chem. Mater. 15 (2003) 1655–1663.
[21] V. Primo-Martin, M. Jansen, J. Solid State Chem. 157 (2001) 76–85.
[22] M.S. Augsburger, M.C. Viola, J.C. Pedregosa, A. Muñoz, J.A. Alonso, R.E. Carbonio, J. Mater. Chem. 15 (2005) 993–1001.
[23] R. Pinacca, M.C. Viola, J.C. Pedregosa, A. Muñoz, J.A. Alonso, J.L. Martínez, R.E. Carbonio, Dalton Trans. (2005) 447–451.
[24] J.-W.G. Bos, J.P. Attfield, Phys. Rev. B 70 (2004) 174434.
[25] A. Mahendra, D.C. Khan, Phys. Rev. B 4 (1971) 3901–3911.
[26] N.S.P. Bhuvanesh, J. Gopalakrishnan, J. Mater. Chem. 7 (1997) 2297–2306.
[27] (a) J.B. Goodenough, Phys. Rev. B 100 (1955) 564;
(b) J.B. Goodenough, J. Phys. Chem. Solids 6 (1958) 287;
(c) J. Kanamori, J. Phys. Chem. Solids 10 (1959) 87.